Printed ISSN 1330–0008
Online ISSN 1333–9125
CD ISSN 1333–8390
CODEN FIZAE4

PHOTOLUMINESCENCE IN CHEMICALLY DEPOSITED (Cd-Zn)S: $CdCl_2$, Ho/Tb FILMS PREPARED AT ROOM TEMPERATURE

SHASHI BHUSHAN[a] and SANDHYA PILLAI[b,1]

[a]*S. O. S. in Physics, Pt. Ravishankar Shukla University, Raipur (C. G.) 492010, India*
Present address: Shri Shankaracharya Engineering College, Junwani, Bhilai (C.G.) 490020, India

[b]*M. P. Christian College of Engineering & Technology, Kailash Nagar, Bhilai (C.G.) 490026, India*

Received 27 November 2008; Revised manuscript received 25 July 2009
Accepted 21 October 2009 Online 27 November 2009

(Cd-Zn)S: $CdCl_2$, Ho/Tb films were prepared by chemical deposition method on glass and Al substrates at room temperature (RT). The films were characterized by SEM, XRD, optical absorption/specular reflectance and photoluminescence (PL) emission spectral studies. SEM studies show the predominance of layered growth along with cluster of particles. XRD studies show crystalline nature of films with maximum intensity corresponding to the (111) plane of CdS cubic phase. Formation of solid solution of the mixed base is also observed. Diffraction lines corresponding to the impurities indicate the substitution of impurities in the lattice. Optical absorption spectra show absorption transitions within the energy levels of impurities. PL emission is most intense in films prepared on Al substrate, which may be due to greater thickness and better crystallinity of such films. PL emission due to transitions within Ho^{3+} as well as Tb^{3+} levels are observed.

PACS numbers: 78.55.Et, 81.15.Lm UDC 52-628, 535.37, 539.216

Keywords: (Cd-Zn)S: $CdCl_2$, Ho/Tb films, photoluminescence, deposition from liquid phases

1. Introduction

The II–VI semiconductors, mainly the cadmium compounds, are very promising materials as their band gaps correspond closely to the visible spectrum. In addition, band-to-band type transitions occurring in these materials make them

[1]Corresponding Author, Tel.: 0788-2242178, E-mail address: madhu_sandhyain@yahoo.com

suitable for applications in many electro-optical devices [1]. The rare earth ions are well known to form efficient luminescent centres as they show distinct absorption and emission transitions within the $4f^N$ shell configuration [2, 3]. Rare earth ion activated phosphors are widely used in fluorescent tubes, colour televisions etc. Thus, addition of these ions as impurities into CdS type materials is quite justified. A number of sophisticated techniques, like vacuum evaporation, sputtering, molecular beam epitaxy etc., were employed by earlier workers [4] for the preparation of films of such materials. However, Bhushan and coworkers [5 – 7] found chemical deposition technique to be simple and economical. They found that films of (Cd-Pb)S:La/Nd/Dy [5, 6] showed a high photo to dark current ratios, sufficiently good PL and moderate photovoltaic efficiency. Similarly, in films of (Zn-Cd)S:Cu,F [7] AC electroluminescence was observed. Mixed base (Cd-Zn)S has a wider band gap than CdS, which makes it suitable for use in phospho-luminescent screens, pigment manufacture etc. [8]. Thus, in the present case (Cd-Zn)S has been selected as base material. Further, holmium and terbium have been used as impurities as they form prospective luminescent materials. Trivalent holmium ion has several energy levels in the energy range from near IR to near UV spectral regions, and many emission and absorption transitions are possible making it suitable for use as a calibration material in molecular absorption spectrophotometry [9]. Similarly, emission from Tb^{3+} ions consists of a series of lines centered on an intense emission near 544 nm and hence is of much interest as a green emitting phosphor [2]. It has wide commercial applications in trichromatic lighting technology and as a probe in biochemistry [10, 11]. $CdCl_2$ has been used as flux which facilitates the incorporation of the rare earth ions into the lattice and also helps in the recrystallisation of (Cd-Zn)S [12]. In our earlier work [13, 14], we have reported PC, PL, XRD and SEM studies of (Cd-Zn)S: $CdCl_2$, Ho/Tb films prepared mainly at 60°C in water bath. It was observed that PL of films prepared at RT showed better emission. The present work concerns with PL studies of (Cd-Zn)S: $CdCl_2$, Ho/Tb films prepared at RT (deposition time 19 hours). Results of SEM, XRD and optical absorption spectra/specular reflectance spectra are also included.

2. *Experimental techniques*

Details of the film preparation are already described in earlier publications [13, 14]. Film thickness was determined by optical interference method and was found to be in the range of 0.6994 – 0.7112 μm for films deposited on glass substrates and in the range of 0.7432 – 0.7545 μm for films deposited on Al substrates. PL excitation source was a 365 nm Hg radiation. PL emission was recorded by an RCA 6217 photo multiplier tube. The optical absorption spectra/reflectance spectra were measured by using a Shimadzu (UV-VIS) Pharmaspec-1700 spectrophotometer. XRD and SEM studies were performed at IUC, DAE Indore using Rigaku RU:H2R Horizontal Rotaflex and JEOL JSM 5600 scanning electron microscope, respectively.

3. Results and discussion

3.1. SEM studies

SEM micrographs of (Cd-Zn)S: $CdCl_2$, Ho and (Cd-Zn)S: $CdCl_2$, Tb films prepared on glass substrates at RT are shown in Figs. 1a and 1b, respectively. In both cases, layered type growth appears. In Fig. 1a, under continued growth, these layers (thickness ~ 230 nm) form a cabbage type structure along with the presence of some voids. In Fig. 1b, scattered leafy type structure is seen. In our earlier publication [14], it has been reported that in Tb-doped films prepared at 60°C in water bath, more ordered layer-type growth, forming balls, appears. Figures 2a and 2b represent the SEM micrographs of (Cd-Zn)S: $CdCl_2$, Ho and (Cd-Zn)S: $CdCl_2$, Tb films prepared on Al substrates, respectively at RT. While Fig. 2a shows the presence of non-uniform distribution consisting of layers (thickness $\sim$ 454 nm) and cluster of particles, Fig. 2b consists of layered structure (thickness $\sim$ 396 nm) in the form of balls.

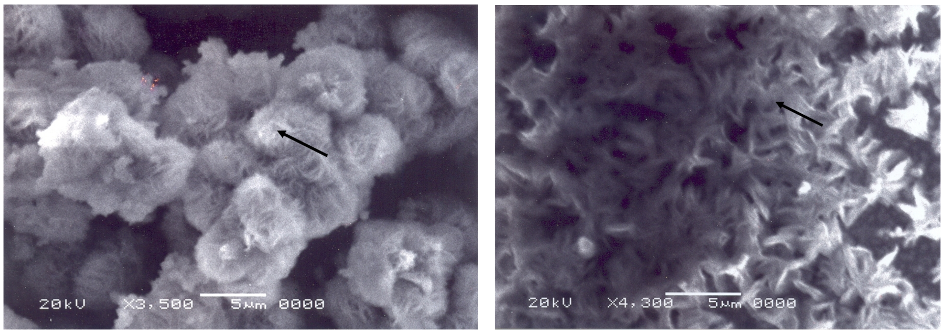

Fig. 1. SEM micrographs of films of (left) ($Cd_{0.8}$-$Zn_{0.2}$)S: $CdCl_2$, Ho*; (right)* ($Cd_{0.8}$-$Zn_{0.2}$)S: $CdCl_2$, Tb *prepared on glass substrates at RT.*

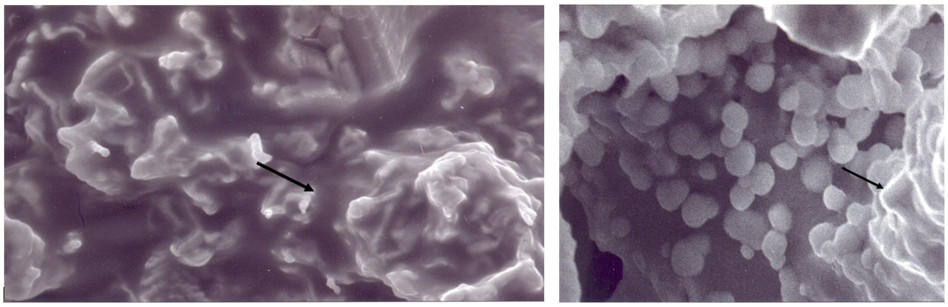

Fig. 2. SEM micrographs of films of (left) ($Cd_{0.8}$-$Zn_{0.2}$)S: $CdCl_2$, Ho*; (right)* ($Cd_{0.8}$-$Zn_{0.2}$)S: $CdCl_2$, Tb *prepared on glass substrates at RT.*

3.2. XRD studies

Figure 3 presents the X-ray diffractogram of ($Cd_{0.8}$-$Zn_{0.2}$)S: $CdCl_2$, Ho film, deposited on glass substrate at RT. The XRD pattern indicates the crystalline nature of the films. The assignments of the different peaks were made by comparison with ASTM data and calculation of lattice constants, which almost matched with the reported values. The corresponding data are presented in Table 1. It is observed that the $(111)_c$ peak of CdS appears with maximum intensity. Other prominent lines correspond to both CdS and ZnS sug-

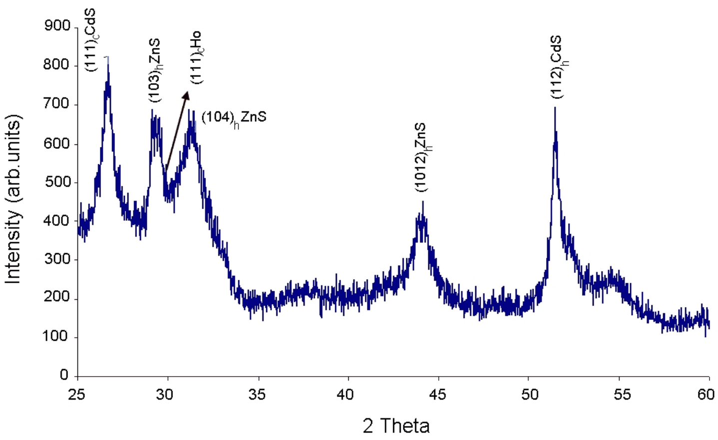

Fig. 3. X-ray diffractogram of ($Cd_{0.8}$-$Zn_{0.2}$)S: $CdCl_2$, Ho *film prepared on glass substrate at RT.*

TABLE 1. XRD data of ($Cd_{0.8}$-$Zn_{0.2}$)S: $CdCl_2$, Ho *film prepared on glass substrate at room temperature.*

d values (Å)		Rel. Intensities		(hkl)	Lattice constant (Å)	
Observed	Reported	Observed	Reported		Observed	Reported
3.3328	3.36	100	100	$(111)_c$CdS	$a = 5.772$	$a = 5.818$
3.0613	3.050	83.6	4	$(103)_h$ ZnS wurtzite (8H)	$a = 3.8214$ $c = 25.13$	$a = 3.82$ $c = 24.96$
2.9793	2.9733	66.3	100	$(111)_c$ Ho	$a = 5.16$	$a = 5.15$
2.8691	2.81	83.3	2	$(104)_h$ ZnS wurtzite (8H)	$a = 3.8214$ $c = 25.83$	$a = 3.82$ $c = 24.96$
2.0487	2.08	54.9	2	$(1012)_h$ ZnS	$a = 3.8214$ $c = 30.84$	$a = 3.82$ $c = 31.20$
1.7732	1.76	84.2	45	$(112)_h$ ZnS	$a = 4.1283$ $c = 6.8341$	$a = 4.1354$ $c = 6.7120$

gesting the formation of a solid solution of (Cd-Zn)S. It is known that different layers of CdS are observed in cubic as well as hexagonal phases. The hexagonal and cubic phases are formed through different atomic arrangements of atomic layers. The hexagonal phase consists of a sequence of atomic layers defined as ABABAB-----, and that of cubic is ABCABCABC-----, [15]. Mixed forms with random stacking of very long period repeats may also be formed, as observed in polytypes of SiC [16]. The total crystal may be considered to be consisting of different atomic layers of CdS in cubic as well as hexagonal phases along with some atomic layers of ZnS in hexagonal phases. According to Langer et al. [17], solid solutions may be thought of as mixtures of microcrystalline regions of pure CdS and ZnS in which each micro-region consists of a number of unit cells of each material with lattice constant of CdS stressed by surrounding ZnS and that of ZnS compressed by its CdS neighbours. These workers also suggested the possibility of solid solution formation consisting of statistical distribution of CdS and ZnS corresponding to their overall concentration. Such a model explains uniform shift of absorption edge with composition [17, 18]. A shift in absorption edge towards shorter wavelength with increase in concentration of ZnS has been reported in our earlier paper [13]. Also, the lattice parameters 'a' and 'c' for different (Cd-Zn) S films prepared on glass substrate at 60°C using water bath at different proportions of CdS to ZnS were calculated using the XRD data [13, 19] and plotted as a function of composition, as shown in Figs. 4a and b, and the corresponding data are presented in Table 2. The values of 'a' and 'c' were found to be decreasing with increasing zinc content. The variations were obeying Vegards law thereby confirming

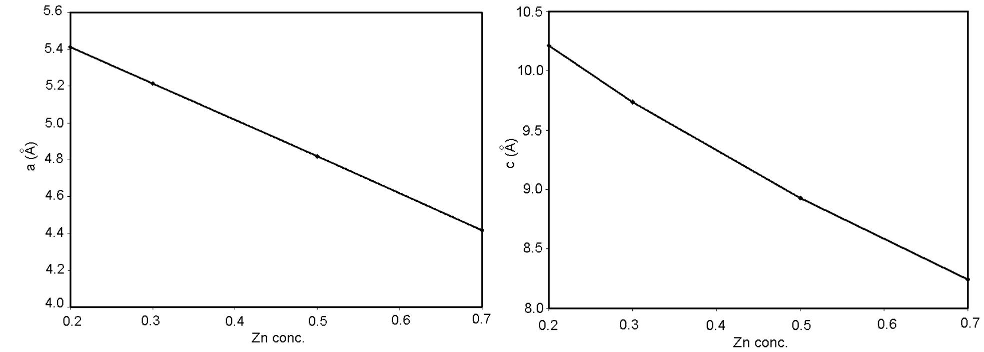

Fig. 4. (left) Variation of lattice constant 'a' with Zn *content; (right) Variation of lattice constant 'c' with* Zn *content.*

the formation of solid solution of the mixed base. Patil et al. [20] have also reported a similar behaviour in screen-printed thick films of (Cd_{1-x}-Zn_x)S prepared by flux technique. The XRD data of different (Cd-Zn)S films prepared at RT are not available at present. However, a similar nature is expected in such films also. On comparing with the XRD data of (Cd-Zn)S films with that of CdS [21], a slight shift in peak positions is observed. Further, absence of some prominent lines of ZnS is also observed. These facts again suggest solid solution formation of (Cd-Zn)S.

TABLE 2. Values of lattice parameters 'a' and 'c' for different (Cd-Zn)S *films prepared on glass substrate at 60°C using water bath.*

Sample	'a' (Å)	'c' (Å)
$(Cd_{0.8}\text{-}Zn_{0.2})S$	5.412	10.213
$(Cd_{0.7}\text{-}Zn_{0.3})S$	5.214	9.736
$(Cd_{0.5}\text{-}Zn_{0.5})S$	4.819	8.928
$(Cd_{0.3}\text{-}Zn_{0.7})S$	4.417	8.242

Further, EDX spectra and the corresponding elemental analysis data for $(Cd_{0.8}\text{-}Zn_{0.2})S$ powders as reported earlier [14] indicate the incorporation of zinc into the lattice in approximately the same proportions. In addition to this, substitution of impurity in the lattice is observed corresponding to the line $(111)_c$ of Ho.

The particle size 'D', the strain value 'ε' and the dislocation density 'δ' were evaluated for the $(111)_c$ peak of CdS by methods reported in earlier publication [14]. These values are summarized in Table 3. The XRD patterns of Tb doped films are already reported in earlier publication [14], which again showed a behavior similar to that of Ho-doped films consisting of diffraction lines of CdS, ZnS and Tb_2O_3. The values of strain and dislocation density are lower in the case of Tb-doped films [14] in comparison to those of films doped with Ho. This may be the reason for the higher PL emission intensity observed in Tb-doped films (stated later).

TABLE 3. Values of particle size (D), strain (ϵ) and dislocation density (δ) for $(Cd_{0.8}\text{-}Zn_{0.2})S\text{: }CdCl_2, Ho$ *film prepared at RT.*

Sample	Particle Size D (nm)	Strain ϵ ($lin^{-2}m^{-4}$)	Dislocation density (10^{15} lin/m^2)
$(Cd_{0.8}\text{-}Zn_{0.2})S\text{: }CdCl_2, Ho$	13.5	0.0054	5.48

3.3. Optical absorption/specular reflectance spectral studies

Figure 5 presents the absorption spectra of different $(Cd_{0.8}\text{-}Zn_{0.2})S$ films deposited on glass substrates at RT. On extrapolation of the plots between $(\alpha h\nu)^2$ vs. $h\nu$ (Taucs plots), for the absorption curves presented in Fig. 5, the values of the band gap have been found to be as follows; 2.41 eV for $(Cd_{0.8}\text{-}Zn_{0.2})S$, 2.44 eV for $(Cd_{0.8}\text{-}Zn_{0.2})S\text{:}CdCl_2$, 2.5 eV for $(Cd_{0.8}\text{-}Zn_{0.2})S\text{:}CdCl_2, Ho$ and 2.43 eV for $(Cd_{0.8}\text{-}Zn_{0.2})S\text{: }CdCl_2, Tb$. In the absorption spectra of Ho-doped film, a broad peak is observed at about 450 nm which is associated to the $^5I_8 \rightarrow {}^5F_1/{}^5G_6$ transition in Ho [22]. Kiryanov et al. [23] have also reported a weak absorption peak in the wavelength range $450 - 500$ nm due to transitions within the Ho^{3+} bands in gadolinium gallium garnet (GGG) crystal co-activated with Yb^{3+} and Ho^{3+}. Also, this

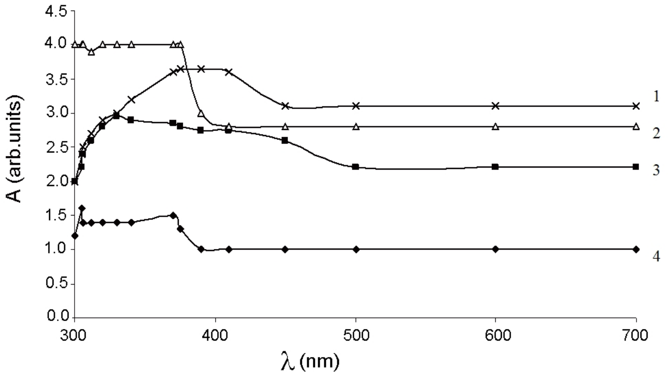

Fig. 5. Absorption spectra of (Cd-Zn)S *films (1)* ($Cd_{0.8}$-$Zn_{0.2}$)S, *(2)* ($Cd_{0.8}$-$Zn_{0.2}$)S: $CdCl_2$, *(3)* ($Cd_{0.8}$-$Zn_{0.2}$)S: $CdCl_2$, Ho, *(4)* ($Cd_{0.8}$-$Zn_{0.2}$)S: $CdCl_2$, Tb, *prepared on glass substrates at RT.*

absorption due to Ho is found to be more prominent for increasing concentrations of NH_4OH (as shown in Fig. 6). In the absorption spectra of Tb-doped films, an absorption peak at 310 nm and another broad peak at 370 nm is observed, which can be related to the transitions $^7F_6(4f^8) \rightarrow 5D_0(5d^14f^7)$ and $^7F_6(4f^8) \rightarrow 5D_3(5d^14f_7)$ transitions, respectively in Tb^{3+} ions [24]. Earlier, in the absorption spectra of Tb-doped films deposited at 60°C [14], the broad peak at 370 nm was not observed. In its oxides, holmium exists only in the +3 valence state [25], while Tb has been known to exist in both +3 and +4 valence states [26]. In the Tb^{4+} state, an absorption peak may be observed in the region 400 – 600 nm [2]. However, in the present work, no peak is observed in this region, thereby suggesting the presence of Tb^{3+} state [14]. The substitution of these trivalent ions (Ho/Tb) in (Cd-Zn)S may take place by creating cation vacancies. The trivalent rare-earth (RE) ions may substitute for divalent Cd/Zn ions forming predominantly pair centers of the type RE^{3+}---(Cd/Zn vacancy)---RE^{3+} [27]. This type of charge compensation seems to be applicable in the present case. Appropriate substitution of anion may also

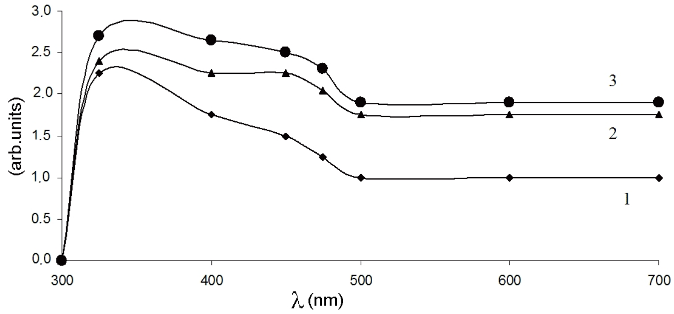

Fig. 6. Absorption spectra of ($Cd_{0.8}$-$Zn_{0.2}$)S: $CdCl_2$, Ho *film deposited at RT and different concentrations of* NH_4OH*: (1) 50%* NH_4OH, *(2) 70%* NH_4OH *and (3) 90%* NH_4OH.

result from Cl ions of $CdCl_2$. But from EDX measurements [14], existence of Cl was not found and hence this possibility is ignored. The overall absorbance has been found to be more in both Ho- and Tb-doped films deposited at RT in comparison to those deposited at 60°C in water bath [13, 14] which may have resulted in better PL intensity (as stated later in Sec. 3.4).

In the case of films deposited on Al substrate, the specular reflectance spectra were studied and the corresponding results are presented in Fig. 7. The reflectance studies of films deposited at 60°C in water bath have been reported earlier [13]. The overall reflectance has been found to be less in Ho- and Tb-doped films deposited at RT, which is in accordance with the increase in absorbance in the films prepared at RT. A lower reflectance is observed at about 450 nm in Ho-doped film, which again accounts for the increase in absorbance observed in this region on glass substrate. In Tb-doped film, lower reflectance is observed at about 350 − 400 nm, which is in accordance with the increase in absorbance in this region. The spikes observed in the wavelength region 300 − 350 nm in all cases may be due to the presence of different materials, but we are unable to relate them to particular elements at present, due to the absence of reflectance data.

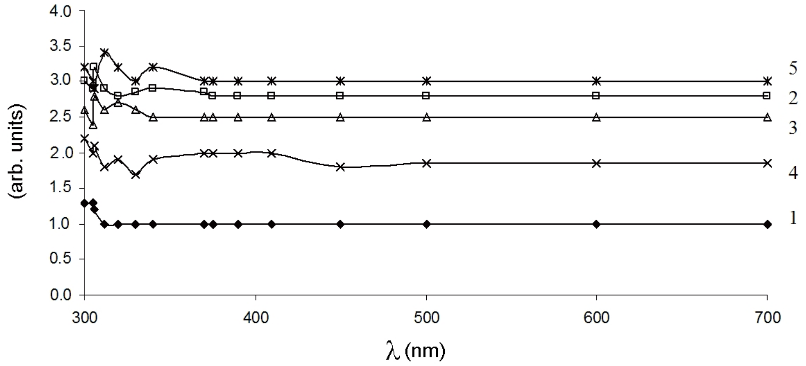

Fig. 7. Specular reflectance spectra of different (Cd-Zn)S *films prepared on Al substrates at RT: (1) Bare* Al *substrate (2)* ($Cd_{0.8}$-$Zn_{0.2}$)S, *(3)* ($Cd_{0.8}$-$Zn_{0.2}$)S: $CdCl_2$, *(4)* ($Cd_{0.8}$-$Zn_{0.2}$)S: $CdCl_2$, Ho, *(5)* ($Cd_{0.8}$-$Zn_{0.2}$)S: $CdCl_2$, Tb.

3.4. PL spectra

The photoluminescence (PL) spectra of different (Cd-Zn)S films deposited at 60°C in water bath on glass and Al substrates have been reported earlier [13, 14]. The corresponding results for the films deposited at RT are presented in this paper. In comparison to the films prepared at 60°C, an increase in the emission intensity is observed in all films deposited at RT. Figure 8 shows the PL emission spectra of different ($Cd_{0.8}$-$Zn_{0.2}$)S films deposited at RT on glass substrates. A shift in peak positions to higher wavelength side (545 nm in the case of Ho-doped film and 546 nm in the case of Tb-doped film) is observed in comparison to that obtained in the case of base material which suggests the substitution of impurity in the lattice.

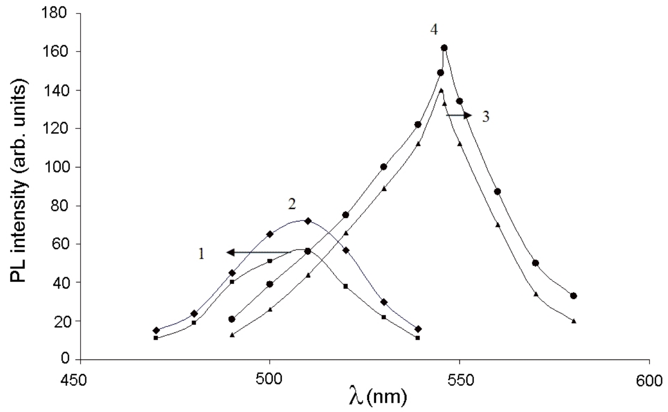

Fig. 8. PL emission spectra of different $(Cd_{0.8}\text{-}Zn_{0.2})S$ *films prepared on glass substrates at RT: (1)* $(Cd_{0.8}\text{-}Zn_{0.2})S$*, (2)* $(Cd_{0.8}\text{-}Zn_{0.2})S\!: CdCl_2$*, (3)* $(Cd_{0.8}\text{-}Zn_{0.2})S\!: CdCl_2, Ho$*, (4)* $(Cd_{0.8}\text{-}Zn_{0.2})S\!: CdCl_2, Tb$.

Maximum emission intensity in Ho- and Tb-doped films prepared at RT is obtained at higher volumes of impurities in comparison to those deposited at 60°C. In the case of Ho-doped film, maximum emission is observed for 6 ml volume of Ho_2O_3 (0.01 M) and in Tb-doped film, maximum emission is observed for 8 ml volume of Tb_2O_3 (0.01 M). At further larger volumes in both cases, emission intensity decreases due to the concentration quenching. Maximum PL intensity in $(Cd_{0.8}\text{-}Zn_{0.2})S$ and $(Cd_{0.8}\text{-}Zn_{0.2})S$: $CdCl_2$ is observed at 510 nm which may be due to the excitonic transitions which are effective in such materials even at room temperature [14, 28]. In the PL spectra of Ho-doped film on glass substrate, maximum intensity observed at 545 nm may be due to the transition from the $^5S_2/^5F_4$ states to the $^5I_8$ ground state of Ho^{3+} [13, 22]. PL emission in Tb-doped films is more intense in comparison to that of Ho-doped films. The maximum PL intensity is observed at 546 nm which may be due to the dominant $^5D_4 \rightarrow ^7F_5$ transition in Tb^{3+} ions [2, 14]. This type of green emission is more prominent in luminescent materials with high Tb^{3+} concentration as cross relaxation produces an increase in the population of $^5D_4$ state at the expense of the $^5D_3$ state [2, 29, 30]. Figure 9 shows the PL spectra of different $(Cd_{0.8}\text{-}Zn_{0.2})S$ deposited at RT on Al substrates. Peak positions obtained in the case of $(Cd_{0.8}\text{-}Zn_{0.2})S$ and $(Cd_{0.8}\text{-}Zn_{0.2})S$: $CdCl_2$ films are the same as those reported in the case of films deposited on glass substrates. However, in the doped films two peaks are observed. In the Ho-doped film, a highly intense peak at 545 nm (as observed in the case of films deposited on glass substrate) and a less intense peak at about 503 nm are observed. They are related to the $^5S_2/^5F_4 \rightarrow ^5I_8$ and $^3H_5 \rightarrow ^5I_8$ transitions in Ho, respectively [22]. In the Tb-doped film, a shoulder is observed at about 490 nm (in addition to the dominant green emission as observed on glass substrate) which may possibly be due to the $^5D_4 \rightarrow ^7F_6$ transition in Tb^{3+} ions [2]. The appearance of additional peaks in the PL spectra of both Ho- and Tb-doped films on Al substrate, in addition to those obtained in the films deposited on glass, is not clearly understood at this stage. It may possibly be due to the formation of

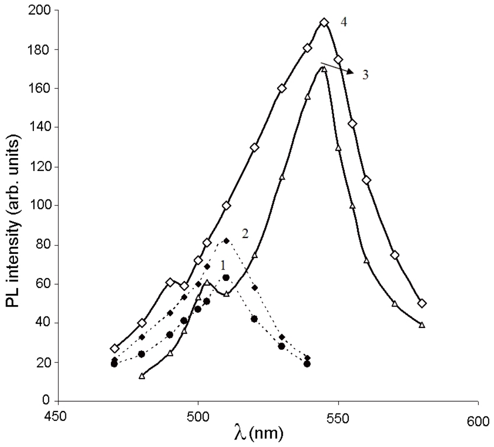

Fig. 9. PL emission spectra of different $(Cd_{0.8}\text{-}Zn_{0.2})S$ *films prepared on* Al *substrates at RT: (1)* $(Cd_{0.8}\text{-}Zn_{0.2})S$*, (2)* $(Cd_{0.8}\text{-}Zn_{0.2})S:CdCl_2$*, (3)* $(Cd_{0.8}\text{-}Zn_{0.2})S:CdCl_2, Ho$*, (4)* $(Cd_{0.8}\text{-}Zn_{0.2})S:CdCl_2, Tb$.

some compound of Al. The overall emission intensity is more on Al substrate in both Ho- and Tb-doped films. This may be due to the greater thickness and improved crystallinity of films deposited on Al substrate. It was already found [13] that XRD studies of films deposited on Al substrates at 60°C show better crystallinity. Bae et al. [31] have also reported superior crystallization and improved photoluminescence by about three times in $[Y_{2-x}Gd_xO_3]$: Eu^{3+} films deposited on Al_2O_3 substrate.

4. Conclusions

Quite intense PL spectra were observed in chemically deposited $(Cd_{0.8}\text{-}Zn_{0.2})S:CdCl_2$, Ho/Tb films prepared on glass and Al substrates at room temperature. PL emission intensity is maximum in films deposited on Al substrate. SEM studies show layered growth and formation of clusters of particles. XRD studies suggest the formation of solid solution of the mixed base. Diffraction lines corresponding to the impurities are also observed indicating the substitution of impurities in the lattice. Absorption studies show transitions within the impurity levels. PL emission in Ho-doped films is related to the $^5S_2/^5F_4 \rightarrow ^5I_8$ and $^3H_5 \rightarrow ^5I_8$ transitions in Ho^{3+} bands. In Tb-doped films, it is related to the dominant $^5D_4 \rightarrow ^7F_5$ and the less intense $^5D_4 \rightarrow ^7F_6$ transition in Tb^{3+} ions.

Acknowledgements

The authors are grateful to IUC DAE, Indore for SEM and XRD studies of the samples. One of the authors (S. P.) is also grateful to Fr. Dr. Abraham Oommen, Exe-Vice Chairman, Dr. R. N. Dash, Director and Prof. K. C. Mani, Administrator of M. P. Christian College of Engineering and Technology, Bhilai for kindly permitting to continue research work at Pt. R. S. U., Raipur (C. G.).

References

[1] L. P. Deshmukh, C. B. Rotti, K. M. Garadkar, P. P. Hankare, B. M. More, D. S. Sutrave and G. S. Shahane, Ind. J. Pure Appl. Phys. **35** (1997) 428.

[2] G. Wakefield, H. A. Keron, P. J. Dobson and J. L. Hutchison, J. Phys. Chem. Solids **60** (1999) 503.

[3] R. Reisfield, T. Saraidarov, E. Ziganski, M. Gaft, S. Lis and M. Pietraszkiewiez, J. Lumin. **102 − 103** (2003) 243.

[4] M. K. Karanjai and D. Dasgupta, Thin Solid Films **150** (1987) 309.

[5] S. Bhushan, M. Mukherjee and P. Bose, J. Mater. Sci. (Materials in Electronics) **13** (2002) 581.

[6] S. Bhushan, S. Shrivastava and A. Shrivastava, J. Mater. Sci. **41** (2006) 7483.

[7] A. Khare and S Bhushan, Cryst. Res. Technol. **41** (2006) 689.

[8] J. D. G. Duran, M. C. Guindo, A. V. Delgado and F. Gonzalez-Caballero, J. Colloid Interface Sci. **193** (1997) 223.

[9] N. Karayianis and D. E. Wortman, J. Phys. Chem. Solids **37** (1976) 675.

[10] T. Yuwei, J. Electric Lighting **4** (2002) 10.

[11] M. Biggiogera and S. Fakan, J. Histo Chemistry and Cyto Chemistry **46** (3) (1998) 389.

[12] R. H. Bube, *Photoconductivity in Solids*, Wiley, New York (1960) p. 161.

[13] S. Bhushan and S. Pillai, Radiat. Eff. **163** (3) (2008) 241.

[14] S. Bhushan and S. Pillai, Cryst. Res. Technol. **43** (7) (2008) 762.

[15] C. Kittel, *Introduction to Solid State Physics* (7th edition), John Wiley and Sons (1995) p. 18.

[16] H. Ibach and H. Luth, *Solid State Physics (An Introduction to Theory and Experiment)*, Springer Int. Student Edition (1991) p. 25.

[17] D. W. Langer, Y. S. Park and R. N. Euwama, Phys. Rev. **152** (2) (1966) 788.

[18] R. S. Singh and S. Bhushan, Chalcogenide Letters **5** (12) (2008) 377.

[19] S. Bhushan and S. Shrivastava, Ind. J. Pure and Appl. Phys. **33** (1995) 371.

[20] L. A. Patil, A. M. Patil and M. S. Wagh, Trends in Applied Sciences Research **1** (4) (2006) 362.

[21] M. Mukherjee and S. Bhushan, Optical Materials **22** (2003) 51.

[22] T. Ishizaka and Y. Kurokawa, J. Lumin. **92** (2000) 57.

[23] A. V. Kiryanov, V. Aboites, A. M. Belovolov, M. J. Damzen, A. Minassian, M. I. Timoshechkin and M. I. Belovolov, J. Lumin. **102 − 103** (2003) 715.

[24] T. R. Matyasiak, M. Gryk, W. Grinberg, Y. S. Lin and R. S. Liu, J. Phys.: Condens. Matter **18** (2006) 10531.

[25] P. Deren, P. Goldner and O. Noel, J. Lumin. **119 − 120** (2006) 38.

[26] B. G. Hyde and T. Leyring, *Rare Earth Research III*. Gordon and Breach, NewYork (1965).

[27] J. Heber, R. Demirbilek and S. I. Nikitin, J. Alloys and Compounds **380** (1-2) (2004) 50.

[28] S. Nam, J. Rhee, O. Byungsung and K. Lee, J. Korean Phys. Soc. **32** (2) (1998) 156.

[29] D. J. Robbins, B. Cockayne, B. Lent and J. L. Clasper, Solid State Commun. **20** (1976) 673.

[30] P. A. M. Berdowski, M. J. J. Lammers and G. Blasse, Chem. Phys. Lett. **113** (1985) 387.

[31] J. S. Bae, K. S. Shim, S. B. Kim, J. H. Jeong, S. S. Yi and J. C. Park, J. Cryst. Growth **264** (2004) 290.

FOTOLUMINESCENCIJA NA SOBNOJ TEMPERATURI KEMIJSKI TALOŽENIH (Cd-Zn)S: $CdCl_2$, Ho/Tb TANKIH SLOJEVA

Tanke slojeve (Cd-Zn)S: $CdCl_2$, Ho/Tb smo pripremali kemijskim taloženjem na staklenu i Al podlogu na sobnoj temperaturi. Te smo slojeve ispitali mjerenjem SEM, XRD, optičke apsorpcije i spektralne odraznosti te fotoluminescentnih emisijskih spectara. Proučavanje SEM pokazuju prevladavanje slojevitog rasta duž nakupina čestica. Mjerenja XRD pokazuju kristaliničnu strukturu slojeva s najjačim vrhom koji odgovara ravnini (111) kubične faze CdS. Opaža se i tvorba čvrste otopine od miješane osnove. Difrakcijske linije od nečistoća ukazuju na zamjene nečistoća u rešetci. Optički apsorpcijski spektri pokazuju apsorpcijske prijelaze među energijskim stanjima nečistoća. Fotoluminescentna emisija je najjača iz slojeva na Al podlozi što je možda posljedica veće debljine i kristaliničnosti tih slojeva. Opažaju se fotoluminescentni prijelazi među stanjima Ho^{3+} i Tb^{3+}.